Unit Commitment with AC Power Flow Constraints for a Hybrid Transmission Grid

L. P. M. I. Sampath*, M. Hotz†, H. B. Gooi‡ and W. Utschick†
*Interdisciplinary Graduate School, Nanyang Technological University, Singapore.
Email: mohashai001@e.ntu.edu.sg
†Department of Electrical and Computer Engineering, Technical University of Munich, Germany.
‡School of Electrical and Electronic Engineering, Nanyang Technological University, Singapore.

***Abstract*—A unit commitment formulation satisfying AC optimal power flow constraints models the resource optimization problem accurately, but is challenging to solve for traditional transmission systems. Integration of generation based on renewable energy sources is often limited by transmission congestion issues in existing grids. For such grids, AC to HVDC conversion schemes are viable and attractive options for capacity expansion. In this respect, we utilize the structural properties of a hybrid AC/HVDC grid architecture with a specific topology to enable an exact mixed integer conic relaxation of the aforementioned problem. The simulation results for the PJM 5-bus system show that the relaxation is exact for the hybrid architecture. Further, it alleviates the network congestion leading to a substantial reduction in generation cost at normal and increased load conditions compared to the reference AC grid. Moreover, the hybrid architecture improves the utilization of the grid to accommodate more demand and generation.**

***Index Terms*—Capacity expansion, convex relaxation, mixed-integer second order cone program, optimal power flow, unit commitment.**

I. Introduction

The transmission system is concerned with the bulk transfer of electrical power from generation facilities to load centers, as generators and loads are in general geographically dispersed. The power system operators (PSOs) attempt to meet the power demand at every time instance using the available power generation resources. This is a challenging task as they need to keep track on three aspects, *i.e.* 1) generator availability and their operational characteristics, 2) security limits of the power system and transmission congestion issues, and 3) demand forecasts and distribution.

The AC optimal power flow (AC-OPF) problem derives the optimum set points for power system variables that satisfy power flow equations, subject to system constraints. For general transmission grids which are meshed in nature, this problem is nonconvex and NP-hard. This nonconvexity mainly lies with the bilinear representation of voltage variables in the power balance equations. DC-OPF is a widely used approach based on a simplified system model. It derives a linear program considering only active power, a unity voltage profile, lossless lines, and small bus voltage angle differences over lines. However, the model mismatch requires more conservative system constraints in a practical implementation, which leads to a suboptimal utilization [1]. In contrast, several convex relaxations are used recently to realize a solution in polynomial time for AC-OPF problems, cf. [2]–[5] and the references therein. However, exactness of these relaxations is only guaranteed under certain conditions which are typically not fulfilled by transmission grids having mesh topologies [2], [4], [6].

Unit commitment (UC) is a decision-making process executed by utilities to ensure minimal cost generation schedules. It results in an optimum generation schedule including the commitment and dispatch for generators. In general, the UC problem does not incorporate the system constraints [7]. Many notable approaches have focused on mixed-integer linear programming (MILP) models with tighter convex hull representations of generator capabilities without network constraints. These UC formulations have been extended to include a linear (DC) representation of the network either with (e.g., [8], [9]) or without (e.g., [10]) real power losses considered.

The complete day-ahead power system economic problem is a combination of UC and OPF problems. Since these two subproblems are individually nonconvex and NP-hard in nature [4], [7], UC with AC-OPF constraints combines the difficulties of both problems and is very challenging to solve [7]. Nevertheless, for example the jump and shift method [11], [12] and outer approximation method [7] address the combined UC and AC-OPF problem. However, both of these approaches are suboptimal and computationally expensive.

Transmission congestion plays a vital role in deciding the order of power dispatch for online generators, as the capacity limitation of some lines can force more expensive generators to dispatch while cheaper generators are not fully utilized. According to the physical laws, the AC power flow over a cycle of branches can stagnate due to congestion of a single branch in the cycle [13]. To reduce the impact of congestion, optimal transmission switching was considered in the literature [13], [14], where transmission line switching is incorporated into the traditional OPF problem to open undesirable lines to increase the utilization of cheaper generation resources. However, this is a combinatorial problem and challenging to

This work is funded by the International Center of Energy Research (ICER), established by Nanyang Technological University (NTU), Singapore and Technische Universität München (TUM), Germany.

realize with AC-OPF constraints [14]. Further, PSOs may be reluctant to use this approach as it causes wearing of breakers and introduces additional transients to the system.

The conventional approach to mitigate transmission congestion is the construction of new lines. However, this is often complicated and protracted by the construction of new corridors due to issues with right of way and public acceptance. In [15]–[17], AC to HVDC transmission line conversion schemes are presented. According to their findings, existing AC transmission lines can be converted to HVDC without corridor adjustments and the active power transmission capacity of the converted HVDC line can be two or more times the apparent power transmission capacity of the existing AC line, depending on the configuration.

Recently a hybrid AC/HVDC transmission grid (HTG) architecture was proposed in [4] as an upgrade methodology for traditional AC transmission grids to enhance utilization and grid loadability. The structural properties of this hybrid architecture provide flexibility in power flow routing and ensure global optimal solvability of the AC-OPF problem under normal operating conditions [5]. Furthermore, it was shown that the hybrid architecture can mitigate the impact of congestion [5] and it constitutes a promising network development approach in case of capacity demands [18].

A. Contributions and Outline

In this study, we extend the system model for HTGs in [4], [5] with time domain constraints to formulate the combined UC and AC-OPF problem to improve the optimal generation schedule over a time horizon in comparison to state-of-art techniques. To this end, in Section II, the OPF subproblem, its convex relaxations and respective conditions for applicability are reviewed. In Section III, the UC problem is reviewed and its computational challenges are discussed. We combine these two subproblems in Section IV. The combined problem results in a mixed-integer nonlinear programming (MINLP) optimization problem that is very hard to solve due to its nonconvex and combinatorial nature. Recently, mixed-integer conic programming (MICP) problems have gained interest, since modern algorithms provide good performance in many engineering problems. This growing demand for MICP solvers has led many commercial software packages such as CPLEX and MOSEK to expand their features and include the technology to solve MICPs. In this work, we utilize the structural properties of the hybrid architecture to relax the multi-period OPF subproblems to convex forms. That enables a reformulation of this MINLP problem into a mixed integer second-order cone programming (MISOCP) problem, which can be solved efficiently using existing conic solvers. Section V presents simulation results for the UC problem satisfying AC-OPF constraints. They illustrate substantial improvements in operational economics and grid utilization with demand growth for the HTG compared to the results for the reference AC grid. In addition, this hybrid architecture supports a flexible integration of additional generation capacity. Section VI concludes the paper.

II. Optimal Power Flow Problem

The OPF problem is a power dispatch optimization problem for a certain time instance that accounts for bus voltage limits and power flow restrictions in the network. In this study, we utilize the HTG model in [4]. We define the variables and parameters which change with time by $(\cdot)^t$ to denote its value at time t. Let $\mathcal{N}$, $\mathcal{L}$, and $\mathcal{H}$ be the set of buses, the set of AC lines, and the set of HVDC lines of the power system respectively, where $|\mathcal{N}| = N$, $|\mathcal{L}| = L$ and $|\mathcal{H}| = H$. To formulate the AC-OPF problem, we use the complex bus voltage vector $v^t \in \mathbb{C}^N$ and HVDC branch flow vector $p^t \in \mathbb{R}_+^H$. A power generation vector is introduced at each bus with a rectangular capability region. For the n^{th} bus $g_n^t = \left[P_n^{\mathrm{G},t},\ Q_n^{\mathrm{G},t}\right]^{\mathrm{T}} \in \mathbb{R}^2$, where $P_n^{\mathrm{G},t}$ is the active and $Q_n^{\mathrm{G},t}$ is the reactive power generation at time t. The generation limits are given by $g_n^{\min} = \left[P_n^{\mathrm{G,min}},\ Q_n^{\mathrm{G,min}}\right]^{\mathrm{T}} \in \mathbb{R}^2$ and $g_n^{\max} = \left[P_n^{\mathrm{G,max}},\ Q_n^{\mathrm{G,max}}\right]^{\mathrm{T}} \in \mathbb{R}^2$. The power demand $d_n^t = \left[P_n^{\mathrm{D},t},\ Q_n^{\mathrm{D},t}\right]^{\mathrm{T}} \in \mathbb{R}^2$ at each bus is taken as fixed at forecast values.

The OPF problem at time t for a system with AC and HVDC lines can be formulated as below. The reader can refer to [4, Section II and Section III] for the exact formulation of the problem from first principles.

$$\min_{v^t,\ p^t,\ g_n^t} \sum_{n\in\mathcal{N}} c_n P_n^{\mathrm{G},t} \tag{1a}$$

$$\text{s. t.}\quad P_n^{\mathrm{G},t} - P_n^{\mathrm{D,t}} = (v^t)^{\mathrm{H}} P_n v^t + h_n^{\mathrm{T}} p^t; \quad \forall n \in \mathcal{N} \tag{1b}$$

$$Q_n^{\mathrm{G},t} - Q_n^{\mathrm{D},t} = (v^t)^{\mathrm{H}} Q_n v^t; \quad \forall n \in \mathcal{N} \tag{1c}$$

$$(v_n^{\min})^2 \le (v^t)^{\mathrm{H}} M_n v^t \le (v_n^{\max})^2; \quad \forall n \in \mathcal{N} \tag{1d}$$

$$(v^t)^{\mathrm{H}} \hat{I}_k v^t \le (I_k^{\max})^2; \quad \forall k \in \mathcal{L} \tag{1e}$$

$$(v^t)^{\mathrm{H}} \check{I}_k v^t \le (I_k^{\max})^2; \quad \forall k \in \mathcal{L} \tag{1f}$$

$$p_l^{\min} \le p_l^t \le p_l^{\max}; \quad \forall l \in \mathcal{H} \tag{1g}$$

$$g_n^{\min} \le g_n^t \le g_n^{\max}; \quad \forall n \in \mathcal{N} \tag{1h}$$

In (1), $(\cdot)^{\mathrm{T}}$ and $(\cdot)^{\mathrm{H}}$ denote the transpose and Hermitian transpose, respectively. $(\cdot)^{\min}$ and $(\cdot)^{\max}$ represent the minimum and maximum values of the corresponding parameters. The objective function (1a) is taken as a linear cost function for generators, where c_n is the marginal cost of generator n. Constraints (1b) and (1c) explain the active and reactive power balance equations at bus n respectively. The matrices P_n and $Q_n \in \mathbb{S}^N$ are functions of the bus admittance matrix for bus n, while $h_n \in \mathbb{R}^H$ describes the power losses (assumed to be proportional to the power flow through HVDC lines) and connectivity of HVDC lines to bus n. Hence, first and second terms of (1b) define AC and HVDC extractions of bus n, respectively. Constraint (1d) explains the bus voltage magnitude limit at bus n characterized by the matrix M_n. Constraints (1e) and (1f) limit the bidirectional current flow through AC line k, where $\hat{I}_k,\ \check{I}_k \in \mathbb{S}^N$ characterize the respective functions of the branch admittance matrix. Power flow limits through HVDC line l and the generation capability at bus n are represented by (1g) and (1h), respectively.

This optimization problem is a nonconvex nonlinear programming problem. However, there exist several mathematical approaches to simplify the complexity in order to support solvability [2]–[6].

A. Semidefinite Relaxation

The formulation in (1) is amenable to semidefinite relaxation (SDR). SDR is based on the cyclic property of the trace operator $\mathrm{tr}(\cdot)$, which facilitates the following reformulation.

$$(v^t)^{\mathrm{H}} X v^t = \mathrm{tr}((v^t)^{\mathrm{H}} X v^t) = \mathrm{tr}(X v^t (v^t)^{\mathrm{H}}) = \mathrm{tr}(XW^t) \quad (2)$$

The quadratic terms in v^t can thus be expressed with linear terms in $W^t = v^t(v^t)^{\mathrm{H}}$. It should be noted that W^t must satisfy two conditions to enable the decomposition into $v^t(v^t)^{\mathrm{H}}$ and, thus, establish equivalence to the AC-OPF problem.

1) W^t must be positive semidefinite (PSD): $W^t \succeq 0$
2) W^t must have rank 1: $\mathrm{rank}\, W^t = 1$

Therein, the AC-OPF problem renders convex in W^t if the rank constraint is eliminated. However, this relaxation is only applicable if the obtained optimizer $(W^t)^\star$ has rank 1. Furthermore, it should be pointed out that the SDR increases the number of variables quadratically [4], [5]. The SDR of the AC-OPF problem at time t is shown in (3).

$$\min_{W^t,\ p^t,\ g_n^t} \sum_{n\in\mathcal{N}} c_n P_n^{\mathrm{G},t} \quad (3a)$$

$$\text{s. t.} \quad P_n^{\mathrm{G},t} - P_n^{\mathrm{D},t} = \mathrm{tr}(P_n W^t) + h_n^{\mathrm{T}} p^t; \quad \forall n \in \mathcal{N} \quad (3b)$$

$$Q_n^{\mathrm{G},t} - Q_n^{\mathrm{D},t} = \mathrm{tr}(Q_n W^t); \quad \forall n \in \mathcal{N} \quad (3c)$$

$$(v_n^{\min})^2 \le \mathrm{tr}(M_n W^t) \le (v_n^{\max})^2; \quad \forall n \in \mathcal{N} \quad (3d)$$

$$\mathrm{tr}(\hat{I}_k W^t) \le (I_k^{\max})^2; \quad \forall k \in \mathcal{L} \quad (3e)$$

$$\mathrm{tr}(\check{I}_k W^t) \le (I_k^{\max})^2; \quad \forall k \in \mathcal{L} \quad (3f)$$

$$p_l^{\min} \le p_l^t \le p_l^{\max}\ ; \quad \forall l \in \mathcal{H} \quad (3g)$$

$$g_n^{\min} \le g_n^t \le g_n^{\max}; \quad \forall n \in \mathcal{N} \quad (3h)$$

$$W^t \succeq 0 \quad (3i)$$

B. Second-Order Cone Relaxation

Power systems are sparsely meshed which renders the constraint matrices of problem (3) sparse. This sparsity pattern of constraint matrices in (3b)-(3f) is defined by the graph of the AC subgrid, i.e. the element (i, j) will only be nonzero if the i^{th} and j^{th} bus of the system is connected by a line. Therefore, many elements in $W^t = (w_{i,j}^t) \in \mathbb{S}^N$ are not to be evaluated. This property can be utilized to reduce the increased dimentionality by relaxing the problem further to a second-order cone program (SOCP). To this end, let AC line k connects bus i to bus j and let $\bar{w}_k^t = \sqrt{2} w_{i,j}^t$ $\big($hence, $(\bar{w}_k^t)^* = \sqrt{2} w_{j,i}^t\big)$. Therewith, the vectorization $\xi : \mathbb{S}^N \to \mathbb{R}^{N+2L}$ of this partial Hermitian matrix is defined as

$$\xi(W^t) = [\, w_{1,1}^t, \ldots, w_{N,N}^t,\ \mathrm{Re}(\bar{w}_1^t), \ldots, \mathrm{Re}(\bar{w}_L^t), \\ \mathrm{Im}(\bar{w}_1^t), \ldots, \mathrm{Im}(\bar{w}_L^t)\,]^{\mathrm{T}} \in \mathbb{R}^{N+2L}. \quad (4)$$

A necessary condition for (3i) is that all 2×2 principal submatrices of W^t are PSD [5]. Thus, (3i) can be relaxed to PSD constraints on active 2×2 principal submatrices. Considering the vectorization $\bar{v}^t = \xi(W^t)$ and $\bar{N} = N + L$, the 2×2 principal submatrix related to AC line k is given by

$$S_k(\bar{v}^t) = \frac{1}{\sqrt{2}} \begin{bmatrix} \sqrt{2}\bar{v}_i^t & \bar{v}_{N+k}^t + \mathrm{j}\bar{v}_{\bar{N}+k}^t \\ \bar{v}_{N+k}^t - \mathrm{j}\bar{v}_{\bar{N}+k}^t & \sqrt{2}\bar{v}_j^t \end{bmatrix} \quad (5)$$

Therewith, the PSD constraint on all active 2×2 principal submatrices is expressed by

$$S_k(\bar{v}^t) \succeq 0; \qquad \forall k \in \mathcal{L}. \quad (6)$$

This second-order cone relaxation (SOCR) reduces the dimentionality of the AC system state representation W^t from N^2 in the SDR to $N + 2L$ real variables in $\bar{v}^t$ in the SOCP [5]. For the SOCR, the semidefinite constraint (3i) is replaced by (6) and the problem is reformulated in $\bar{v}^t$, which results in the following optimization problem:

$$\min_{\bar{v}^t,\ p^t,\ g_n^t} \sum_{n\in\mathcal{N}} c_n P_n^{\mathrm{G},t} \quad (7a)$$

$$\text{s. t.} \quad P_n^{\mathrm{G},t} - P_n^{\mathrm{D},t} = \xi(P_n^{\mathrm{T}})^{\mathrm{T}} \bar{v}^t + h_n^{\mathrm{T}} p^t; \quad \forall n \in \mathcal{N} \quad (7b)$$

$$Q_n^{\mathrm{G},t} - Q_n^{\mathrm{D},t} = \xi(Q_n^{\mathrm{T}})^{\mathrm{T}} \bar{v}^t; \quad \forall n \in \mathcal{N} \quad (7c)$$

$$(v_n^{\min})^2 \le \xi(M_n^{\mathrm{T}})^{\mathrm{T}} \bar{v}^t \le (v_n^{\max})^2; \quad \forall n \in \mathcal{N} \quad (7d)$$

$$\xi(\hat{I}_k^{\mathrm{T}})^{\mathrm{T}} \bar{v}^t \le (I_k^{\max})^2; \quad \forall k \in \mathcal{L} \quad (7e)$$

$$\xi(\check{I}_k^{\mathrm{T}})^{\mathrm{T}} \bar{v}^t \le (I_k^{\max})^2; \quad \forall k \in \mathcal{L} \quad (7f)$$

$$p_l^{\min} \le p_l^t \le p_l^{\max} \quad \forall l \in \mathcal{H} \quad (7g)$$

$$g_n^{\min} \le g_n^t \le g_n^{\max}; \quad \forall n \in \mathcal{N} \quad (7h)$$

$$S_k(\bar{v}^t) \succeq 0; \quad \forall k \in \mathcal{L} \quad (7i)$$

C. Hybrid AC/HVDC Grid Architecture

The SOCR (7) of (1) is exact if the solution permits a PSD rank-1 completion. For a conventional transmission grid, this is typically not the case [5]. The hybrid architecture proposed in [4], which comprises a radial AC subgrid with additional HVDC lines, supports the exactness of the SOCR, *i.e.*, it enables the PSD rank-1 completion under normal operating conditions as shown in [5]. For this reason, the SOCP in (7) can be utilized instead of the nonconvex problem in (1) to determine the OPF. Concluding, it shall be noted that the bus voltage vector can be recovered using the tree traversal method given in [19, Sec. III-B-3]. The solution quality or the exactness of relaxation can be measured by the *relaxation error measures* (mean error, $\kappa(\tilde{V}^\star)$ and maximum error, $\bar{\kappa}(\tilde{V}^\star)$) in [5, Sec. VI-C], which quantify the relative error of the reconstructed voltage phasors.

III. Unit Commitment

A. Objective Function and Generator Capability Constraints

Let $\mathcal{T}$ be the set of time instances for the horizon considered in the optimization problem, where T is the number of time instances such that $T = |\mathcal{T}|$. UC minimizes the generation cost as in (7a) for the considered time horizon $\mathcal{T}$. Furthermore, the cost model considers the startup cost α_n and the shutdown cost β_n, in addition to the generation cost c_n. A binary variable u_n^t is used to indicate the commitment of generator n at time

instance $t \in \mathcal{T}$. When generator n is committed to operate at time instance t, u_n^t will take 1 and it will be 0 otherwise. Two separate binary variables are introduced for the startup and shutdown instances of each generator denoted by su_n^t and sd_n^t, respectively. The relationship of these binary variables are presented in (8) and the generator power injection constraints in (1h) are modified as in (9).

$$su_n^t - sd_n^t = u_n^t - u_n^{t-1};\ \forall n \in \mathcal{N},\ \forall t \in \mathcal{T}\backslash\{1\} \quad (8)$$

$$u_n^t g_n^{\min} \le g_n^t \le u_n^t g_n^{\max};\ \forall n \in \mathcal{N},\ \forall t \in \mathcal{T} \quad (9)$$

Therewith, the capability of generator n will be switched between zero and the rectangular injection domain depending on the commitment state u_n^t at time t.

B. Minimum Uptime and Downtime Constraints

Once a generator is committed to operate at the time instance t, it will be kept in operation for the interval $[t,\ t + T_n^{\mathrm{U}} - 1]$, where T_n^{U} is the minimum uptime for the generator n. Similarly, once a generator is shutdown at the time instance t, it will be kept idle for the interval $[t,\ t + T_n^{\mathrm{D}} - 1]$, where T_n^{D} is the minimum downtime for generator n. This is related to the lifetime assurance of the generators. It is implemented by following two constraints.

$$\sum_{\tau=t}^{t+T_n^{\mathrm{U}}-1} u_n^\tau \ge T_n^{\mathrm{U}} su_n^t; \qquad \forall n \in \mathcal{N},\ \forall t \in \mathcal{T} \quad (10)$$

$$\sum_{\tau=t}^{t+T_n^{\mathrm{D}}-1} [1 - u_n^\tau] \ge T_n^{\mathrm{D}} sd_n^t; \qquad \forall n \in \mathcal{N},\ \forall t \in \mathcal{T} \quad (11)$$

C. Generator Ramp Constraints

Ramp constraints are intertemporal, which can be classified into three types: 1) operating ramp constraints, 2) startup ramp constraints, and 3) shutdown ramp constraints [20]. Operating ramp constraints restrict the maximum rate of change of active power generation of a generator at two consecutive time instances. The up-ramp rate R_n^{U} and down-ramp rate R_n^{D} are constants that govern the maximum power increment and decrement capability of generator n. The startup ramp constraint limits the initial power dispatch just after commitment and the shutdown ramp constraint limits the final power dispatch just before decommitment. In general, the minimum power output is considered as both startup and shutdown ramp limit for a generator. The ramp constraints are expressed in (12) and (13).

$$P_n^{\mathrm{G},t} - P_n^{\mathrm{G},t-1} \le u_n^{t-1} R_n^{\mathrm{U}} + \left(1 - u_n^{t-1}\right) P_n^{\mathrm{G,min}};\ \forall n \in \mathcal{N},\ \forall t \in \mathcal{T}\backslash\{1\} \quad (12)$$

$$P_n^{\mathrm{G},t-1} - P_n^{\mathrm{G},t} \le u_n^{t} R_n^{\mathrm{D}} + \left(1 - u_n^{t}\right) P_n^{\mathrm{G,min}};\ \forall n \in \mathcal{N},\ \forall t \in \mathcal{T}\backslash\{1\} \quad (13)$$

IV. Unit Commitment with AC Power Flow Constraints

As discussed in Section I, the complete power system optimization problem constitutes a co-optimization of UC and AC-OPF problems. It is an MINLP that can be formulated as follows:

$$\min_{\substack{v^t,\ p^t,\ g_n^t,\\ u_n^t,\ su_n^t,\ sd_n^t}} \sum_{t\in\mathcal{T}} \sum_{n\in\mathcal{N}} \left[c_n P_n^{\mathrm{G},t} + \alpha_n su_n^t + \beta_n sd_n^t\right] \quad (14a)$$

$$\text{s. t. } (8) - (13) \quad (14b)$$

$$(1\mathrm{b}) - (1\mathrm{g}); \qquad \forall t \in \mathcal{T} \quad (14c)$$

where (14b) and (14c) represent the constraints of the UC subproblem and the AC-OPF subproblems, respectively. In this formulation, (9) replaces (1h) in the original AC-OPF problem (1).

This is an extensive nonconvex and combinatorial problem which is difficult to solve. Therefore, the most common practical approach is the linearization of the OPF subproblem using the DC-OPF model [9]. This simplifies the problem (14) to a MILP which is computationally tractable. However, the results may not be feasible for direct implementation due to the lack of model accuracy, *i.e.* slack power capability, power flow, or voltage limit violations may occur. Then, the MILP must be adapted, for example, with reduced flow limits at violated time instances and solved iteratively. Although this process may provide feasible results after some iterations, there is no prior guarantee. Moreover, the feasible utilization may be suboptimal or the process may fail to find a feasible solution due to improper modifications.

The UC subproblem in (14) is NP-hard to solve due to the binary variables involved in the model which are not possible to omit. For this reason, we propose to reformulate the AC-OPF subproblem using the convex relaxation (7) presented in Section II-B. Therewith, the UC problem with AC-OPF constraints can be formulated as follows.

$$\min_{\substack{\bar{v}^t,\ p^t,\ g_n^t,\\ u_n^t,\ su_n^t,\ sd_n^t}} \sum_{t\in\mathcal{T}} \sum_{n\in\mathcal{N}} \left[c_n P_n^{\mathrm{G},t} + \alpha_n su_n^t + \beta_n sd_n^t\right] \quad (15a)$$

$$\text{s. t. } (8) - (13) \quad (15b)$$

$$(7\mathrm{b}) - (7\mathrm{g}),\ (7\mathrm{i}); \qquad \forall t \in \mathcal{T} \quad (15c)$$

In problem (15), when all binary variables are fixed, the remaining multi-period AC-OPF problem is a SOCP problem. This way problem (14) can be cast as a MISOCP problem which extensively reduces computational burden, without compromising actual electrical model accuracy. However, the solution of the problem (15) is recoverable only if the SOCR is exact (see Section II). Conventional AC grids typically do not meet these necessary conditions for relaxation tightness [5]. In this respect, the hybrid architecture in [4] supports the exactness as follows.

Binary variables in problem (15) decide the generator commitment which modifies injection capability regions of buses at each time instance as in (9), while satisfying intertemporal constraints (12) and (13). However, for any binary variable combination the modified injection regions are still polyhedral sets which satisfy the assumptions in [5]. Therefore, for any fixed binary variable configuration in (15), it will be T different AC-OPF problems for which the SOCR is exact,

supported by the particular topology of the hybrid architecture as shown in [5]. Therefore, the hybrid architecture allows to optimize operational resources efficiently using state-of-art MISOCP solvers like MOSEK and CPLEX. Further, it supports the accurate planning and analysis of the necessary system expansion measures by directly solving the complete day-ahead optimization problem.

V. Simulation Results and Discussion

In this section, we present three case studies to illustrate the proposed method and compare the performance of the upgraded HTG and the reference AC grid (ACG). The optimization problems for both ACG and HTG were programmed in MATLAB and solved through the YALMIP interface [21].

A. Test System

The numerical studies were conducted for the PJM 5-bus test system in [22], which is shown in Figure 1(a). The system is modified as in [4] and considered as the reference ACG in the study. The HTG is shown in Figure 1(b). The details about the conversion can be found in [4, Sec. VI-A]. It has a radial AC subgrid comprising four lines that span all buses. Two lines are converted to HVDC lines.

The minimum active power capability of the three generators are taken as $20\mathrm{MW}$, $1\mathrm{MW}$, and $40\mathrm{MW}$ respectively. Both, up-ramp and down-ramp rates are taken as $105\mathrm{MW/h}$, $260\mathrm{MW/h}$, and $300\mathrm{MW/h}$ (*i.e.* half of the maximum power per hour) for each generator, respectively. The minimum uptime and downtime for each generator are taken as $\{6, 3\}\mathrm{h}$, $\{1, 1\}\mathrm{h}$ and $\{10, 6\}\mathrm{h}$, respectively. The startup cost and shutdown cost for every generator are taken as \$100 and \$10, respectively. The load profile for an exemplary day $(24\mathrm{h})$ is considered in this study, which is available in [23, Table IV]. The peak active power demand of the system is adjusted to $1000\mathrm{MW}$, which is the total demand of the PJM 5-bus system [22] and the total demand at other time instances is scaled proportionally. Similarly, peak reactive power demand is taken as $330\mathrm{Mvar}$ and assumed to have the same variation as the active demand profile considering the power factor to be constant. Individual demand at each bus is assumed to be varied in proportion to the given values in [22] at each hour.

B. Numerical Simulations

1) ACG: As discussed in Section I, the optimization problem of UC with AC-OPF constraints for ACG is a MINLP which is very challenging to solve. Therefore, we follow the steps mentioned below to compute an AC power flow feasible generation schedule for the ACG.

Step 1: Solve the UC problem with DCOPF constraints.
Step 2: Execute an AC power flow simulation.
Step 3: Check the solution for feasibility.
Step 4: Perform feasibility restoration.

In Step 1, we formulate the UC problem with DCOPF constraints as a MILP and solve it using CPLEX. Then, this solution is used in Step 2 to execute an AC power flow simulation using MATPOWER [24]. Here, we fix the commitment and the active power dispatch of generators, while the voltage inputs for generators are given as $1\mathrm{p.u.}$ (mid-point of the feasible region). If the solution exceeds the reactive power limits of PV buses, the power flow program will convert the respective PV buses to PQ buses (by keeping reactive power outputs at their upper or lower limits, correspondingly) and solve for voltage variables. The power flow simulation provides the slack power need to compensate the power losses. Subsequently, in Step 3 the feasibility of the Step 2 solution is checked for the compliance with power flow limits and variable bounds. If it is feasible, we exit from the algorithm taking the Step 2 solution as the optimal solution. If not, we tighten the corresponding limits by 1% in Step 4 (only at the respective time instances) and return to Step 1 in the algorithm. If the MILP problem in Step 1 becomes computationally infeasible at some point in the iterative process, then we assume the ACG does not have a feasible solution for the optimization problem.

2) HTG: As discussed in Section IV, the UC with AC-OPF constraints for the HTG is formulated as the MISOCP problem (15). It is solved using MOSEK through YALMIP [21].

C. Case Study 1: Economic Operation

In this test case, we study the economic performance of the two grid architectures at the nominal demand. For the reference ACG, the solution procedure took nine iterations (*i.e.* the MILP problem was solved using adapted limits) to compute the feasible solution. The total generation cost for the reference ACG is $\$298{,}793/\mathrm{day}$. For the HTG, it reduces to $\$260{,}560/\mathrm{day}$ which is a 12.80% reduction.

Figure 2(a) and Figure 2(b) depict the optimal power dispatch of the HTG and the reference ACG respectively. As per marginal cost factors of generators in the system, the *merit-order-of-dispatch* should be Unit 3 $(\$10/\mathrm{MWh})$ at bus $5 \rightarrow$ Unit 1 $(\$14/\mathrm{MWh})$ at bus $1 \rightarrow$ Unit 2 $(\$30/\mathrm{MWh})$ at bus 3. It can be observed that the power dispatch for the ACG during the peak period deviates from this merit order due to transmission congestion. This results in an increase of generation cost for the ACG. In contrast, the power dispatch for the HTG is following this merit order as shown in Figure 2(a), which is reflected by cost savings. Thus, the hybrid architecture alleviates the congestion effectively.

Figure 3 shows the power losses for the two systems. It can be observed that the HTG results in more losses out of which HVDC subgrid accounts for $25\% - 40\%$. In the ACG, active power generation is more distributed, while in the HTG, it is concentrated at Unit 3 at bus 5. This decreases the total generation cost, however since Unit 3 is remote from the load center, power losses increase.

D. Case Study 2: Grid Loadability

In this case study, we examine the ability of the two systems to accommodate a growing demand. To this end, we scale up the load profile by a demand growth factor σ, *i.e.* $d_n^t \rightarrow (1+\sigma)\, d_n^t;\ \forall n \in \mathcal{N},\ \forall t \in \mathcal{T}$. Table I reports the total generation cost at different system loads for both grids and the

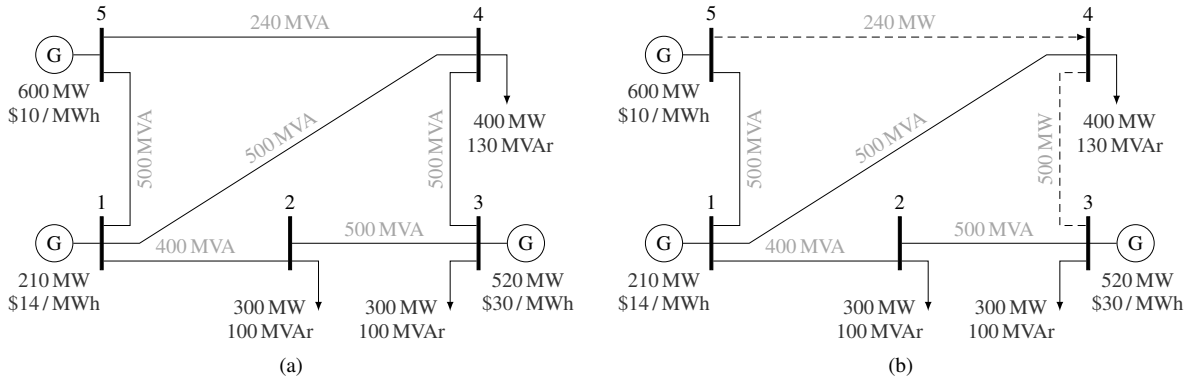

Figure 1. Single-line diagrams of the adapted PJM system (cf. [22]), where (a) is the original ACG and (b) is the HTG obtained by upgrading AC line $3-4$ and $5-4$ to HVDC. Note that (unidirectional) HVDC lines are represented by a (directional) dashed line [4, Fig. 1].

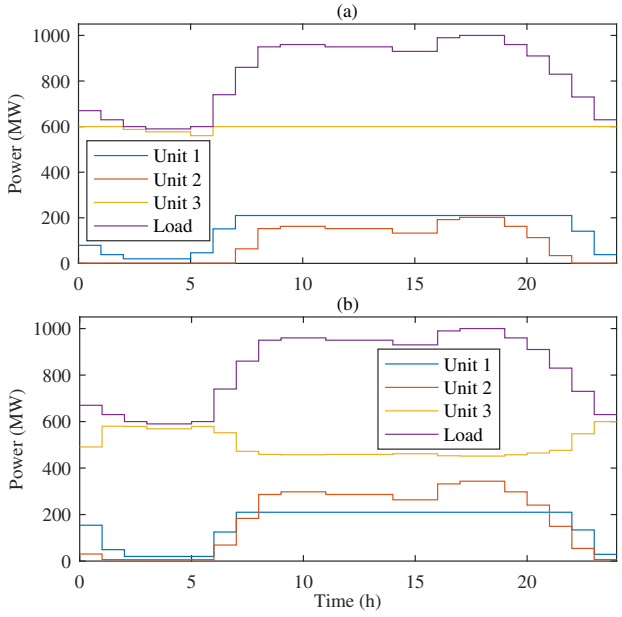

Figure 2. Power dispatch schedule for (a) the HTG and (b) the ACG.

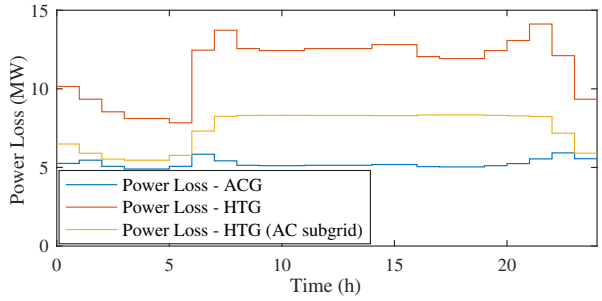

Figure 3. Losses of the ACG and HTG (with and without HVDC losses).

relative cost reduction resulting from the hybrid architecture compared to the reference ACG at each load demand.

The HTG offers consistent economic benefits for growing demand in comparison to the ACG. The ACG can accommodate an increase of up to 14% which utilizes up to 86% of the active power generation capacity. In contrast, the HTG can serve up to 31% more load at which it exploits almost all the active power generation capacity (99.48%) to satisfy the load while accounting for losses.

TABLE I
ECONOMIC EFFICIENCY WITH GRID LOADABILITY

Demand Growth Factor (σ)	Total Cost ($/day)		Cost Reduction
	ACG	HTG	
5%	327,190	285,502	12.74%
10%	355,806	311,090	12.57%
14%	382,083	332,168	13.06%
31%	–	424,577	–

E. Case Study 3: Generation Expansion

In this case study, we further investigate the loadability of these two systems with an increase of generation capacity. To analyze the flexibility in expansion, we separately expand each generation facility in the system by 250MW. The load demand is increased proportionally at every load bus analogous to Case Study 2. The utilization of the total generation and the maximum possible additional demand that can be supplied are documented in Table II.

TABLE II
GENERATION EXPANSION CAPABILITY

Bus	ACG		HTG	
	Generation Utilization	Load Increase	Generation Utilization	Load Increase
1	76.93%	21%	99.39%	55%
3	85.78%	35%	99.77%	56%
5	72.46%	14%	92.24%	44%

The results indicate that the HTG facilitates approximately uniform generation expansion capability at every location (bus) in the grid. This provides flexibility to increase the hosting capacity for remote generation facilities such as renewable energy generation. Furthermore, the hybrid architecture can be

a possible solution to accommodate demand growth as it can support between $44\% - 56\%$ more load, without introducing additional lines to the system. In comparison, the generation utilization is poor in the reference ACG and transmission capacity expansion is necessary to utilize the available generation resources. Concluding, Figure 4 shows that the relaxation errors of the SOCR are minor and acceptable for all simulation runs in the three case studies.

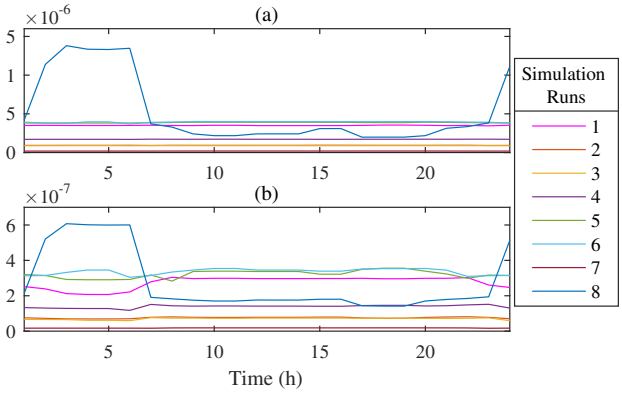

Figure 4. Relaxation error at each hour for all simulation runs: 1 for Case Study 1, $2-5$ for Case Study 2 (order as in Table I), and $6-8$ for Case Study 3 (order as in Table II), where (a) is the maximum error $(\bar{\kappa}(\tilde{V}^\star))$ and (b) is the mean error $(\kappa(\tilde{V}^\star))$.

VI. Conclusion

This paper provides the electrical system model and mathematical foundation to formulate the UC problem with AC power flow constraints as a MISOCP problem. Tightness of the relaxation is guaranteed by the hybrid architecture. This method provides accurate system modeling for flow based day-ahead market coupling while relieving the computational burden, where the latter is similar to the traditional MILP-based approaches. On the other hand, the hybrid architecture provides several operational benefits. The simulation results show that generators are dispatched closely to their merit order, reducing the cost of generation by approximately 13% at nominal and high load conditions, compared to ACG. However, power losses may increase depending on the distribution of generation and load in the system. Furthermore, it is shown that more than 92% of expanded generation can be utilized while increasing the grid loadability by more than 44%, regardless of the location, where the ACG performs significantly worse in all these aspects. Thus, the hybrid architecture can potentially serve an increased demand in the future and support the flexible integration of remote generation.

References

[1] F. Li and R. Bo, "DCOPF-based LMP simulation: Algorithm, comparison with ACOPF, and sensitivity," *IEEE Transactions on Power Systems*, vol. 22, no. 4, pp. 1475–1485, Nov. 2007.

[2] S. H. Low, "Convex relaxation of optimal power flow-Part I: Formulations and equivalence," *IEEE Transactions on Control of Network Systems*, vol. 1, no. 1, pp. 15–27, March 2014.

[3] ——, "Convex relaxation of optimal power flow-Part II: Exactness," *IEEE Transactions on Control of Network Systems*, vol. 1, no. 2, pp. 177–189, June 2014.

[4] M. Hotz and W. Utschick, "A hybrid transmission grid architecture enabling efficient optimal power flow," *IEEE Transactions on Power Systems*, vol. 31, no. 6, pp. 4504–4516, Nov 2016.

[5] ——, "The hybrid transmission grid architecture: Benefits in nodal pricing," *IEEE Transactions on Power Systems*, vol. 33, no. 2, pp. 1431–1442, March 2018.

[6] R. Madani, S. Sojoudi, and J. Lavaei, "Convex relaxation for optimal power flow problem: Mesh networks," *IEEE Transactions on Power Systems*, vol. 30, no. 1, pp. 199–211, Jan 2015.

[7] A. Castillo, C. Laird, C. A. Silva-Monroy, J. P. Watson, and R. P. O'Neill, "The unit commitment problem with ac optimal power flow constraints," *IEEE Transactions on Power Systems*, vol. 31, no. 6, pp. 4853–4866, Nov 2016.

[8] L. Wu and M. Shahidehpour, "Accelerating the benders decomposition for network-constrained unit commitment problems," *Energy Systems*, vol. 1, no. 3, pp. 339–376, 2010.

[9] J. M. Morales, A. J. Conejo, and J. Perez-Ruiz, "Economic valuation of reserves in power systems with high penetration of wind power," *IEEE Transactions on Power Systems*, vol. 24, no. 2, pp. 900–910, May 2009.

[10] M. J. Feizollahi, M. Costley, S. Ahmed, and S. Grijalva, "Large-scale decentralized unit commitment," *International Journal of Electrical Power & Energy Systems*, vol. 73, pp. 97–106, 2015.

[11] S. X. Chen and H. B. Gooi, "Jump and shift method for multi-objective optimization," *IEEE Transactions on Industrial Electronics*, vol. 58, no. 10, pp. 4538–4548, Oct 2011.

[12] L. P. M. I. Sampath, A. Krishnan, K. Chaudhari, H. B. Gooi, and A. Ukil, "A control architecture for optimal power sharing among interconnected microgrids," in *2017 IEEE Power Energy Society General Meeting*, July 2017, pp. 1–5.

[13] P. A. Ruiz, J. M. Foster, A. Rudkevich, and M. C. Caramanis, "Tractable transmission topology control using sensitivity analysis," *IEEE Transactions on Power Systems*, vol. 27, no. 3, pp. 1550–1559, Aug 2012.

[14] B. Kocuk, S. S. Dey, and X. Sun, "New formulation and strong MISOCP relaxations for AC optimal transmission switching problem," *IEEE Transactions on Power Systems*, vol. PP, no. 99, pp. 1–1, 2017.

[15] B. Sander, J. Lundquist, I. Gutman, C. Neumann, B. Rusek, and K. Weck, "Conversion of AC multi-circuit lines to AC-DC hybrid lines with respect to the environmental impact," *Cigre Session, Paris*, 2014.

[16] J. Lundkvist, I. Gutman, and L. Weimers, "Feasibility study for converting 380 kV AC lines to hybrid AC/DC lines," in *Proc. EPRI's High-Voltage Direct Current & Flexible AC Transmission Systems Conference*, 2009, p. 11.

[17] ABB Grid Systems, "HVDC Light – It's time to connect," ABB AB, Ludvika, Sweden, Tech. Rep., Dec. 2012.

[18] M. Hotz, I. Boiarchuk, D. Hewes, R. Witzmann, and W. Utschick, "Reducing the need for new lines in Germany's energy transition: The hybrid transmission grid architecture," in *International ETG Congress 2017*, accepted. [Online]. Available: http://arxiv.org/abs/1707.07946

[19] B. Subhonmesh, S. H. Low, and K. M. Chandy, "Equivalence of branch flow and bus injection models," in *Proc. 50th Annual Allerton Conference on Communication, Control, and Computing (Allerton)*, Oct 2012, pp. 1893–1899.

[20] J. M. Arroyo and A. J. Conejo, "Modeling of start-up and shut-down power trajectories of thermal units," *IEEE Transactions on Power Systems*, vol. 19, no. 3, pp. 1562–1568, Aug. 2004.

[21] J. Löfberg, "YALMIP : A toolbox for modeling and optimization in MATLAB," in *Proc. CACSD Conference*, Taipei, Taiwan, 2004.

[22] F. Li and R. Bo, "Small test systems for power system economic studies," in *Proc. IEEE PES General Meeting*, July 2010, pp. 1–4.

[23] Reliability Test System Task Force, "The ieee reliability test system-1996. a report prepared by the reliability test system task force of the application of probability methods subcommittee," *IEEE Transactions on Power Systems*, vol. 14, no. 3, pp. 1010–1020, Aug 1999.

[24] R. D. Zimmerman, C. E. Murillo-Sanchez, and R. J. Thomas, "MATPOWER: Steady-state operations, planning, and analysis tools for power systems research and education," *IEEE Transactions on Power Systems*, vol. 26, no. 1, pp. 12–19, Feb 2011.